

## Two-photon photochromism of two simple chromene derivatives

Minghui Hu<sup>a</sup>, Susumu Kawauchi<sup>a,\*</sup>, Mitsuru Satoh<sup>a</sup>, Jiro Komiyama<sup>a</sup>,  
Junji Watanabe<sup>a</sup>, Seiya Kobatake<sup>b</sup>, Masahiro Irie<sup>b</sup>

<sup>a</sup> Department of Organic and Polymeric Materials, Tokyo Institute of Technology, O-okayama 2-12-1, Meguro-ku, Tokyo 152-8552, Japan

<sup>b</sup> Department of Chemistry and Biochemistry, Kyushu University, Hakozaki 6-10-1, Higashi-ku, Fukuoka 812-8581, Japan

Received 23 July 2001; received in revised form 4 March 2002; accepted 11 March 2002

### Abstract

Two kinds of typical chromene derivatives, 5a,9-dimethyl-5aH-benzo[b]chromene (**1**) and 7a,11-dimethyl-7aH-dibenzo[b,f]chromene (**2**), were synthesized to understand the relationship between molecular structures and two-photon photochromism for chromene derivatives. The photochromic performances of **1** and **2** in hexane were investigated by measuring ultraviolet (UV)–visible absorption and <sup>1</sup>H nuclear magnetic resonance spectral changes upon UV irradiation. The results indicate that **1** showed the two-photon photochromic reaction, whereas the main photochemical reaction of **2** was the isomerization between the open-*E* and open-*Z* isomers. Density functional theory (DFT) calculations suggest that these different photochromic performances are attributed to the differences in relative stabilities of closed, open-*Z* and open-*E* isomers for **1** and **2**. Combined with DFT calculations for 12aH-12a-methyl-naphtho[3,2]chromene (**3**), the most typical chromene derivative well exhibiting two-photon photochromism, we conclude that chromene derivatives show the best two-photon photochromic performances only if closed isomers are more stable than open-*Z* and open-*E* isomers. © 2002 Elsevier Science B.V. All rights reserved.

**Keywords:** Photochromism; Chromene; Relative energy; Density functional theory; Transient absorption

### 1. Introduction

Photochromism is defined as a reversible transformation of a chemical species between two isomers that have different optical properties upon photoirradiation [1]. Photochromic compounds that reversibly change their optical properties upon photoirradiation are potentially applicable to various photoelectronic devices, such as optical memory and switches [2–7]. For these applications, the non-destructive readout is indispensable.

Over recent years, two approaches have been pursued in an effort to realize the non-destructive readout. One is to employ photochromic compounds that have a reaction threshold during photoisomerization [8–10]. The other is to develop two-photon photochromic systems in which photoirradiation strength and wavelengths are precisely controlled [11]. Some chromene (i.e., 2*H*-benzopyran) derivatives show such two-photon photochromism [12–14]. Their photochromic reactions proceed between two isomers via an unstable intermediate in a two-step, two-photon process, as shown in Fig. 1. The recording can be carried out by using a strong beam that converts closed isomers to bicyclo isomers via keto intermediates (i.e., open-*Z* isomers)

with the two-photon mechanism. Although bicyclo isomers are thermodynamically unstable, inferred from their highly steric structures, they are stable at room temperature as soon as produced, because of the large activation energy needed for the thermal transformation from bicyclo to open-*Z* isomers. The intermediate open-*Z* isomers, however, are unstable at room temperature and readily return to closed isomers via thermal reaction. Therefore, closed isomers do not convert to bicyclo isomers by using a weak beam during the reading process, thereby realizing the non-destructive readout. In addition, bicyclo isomers have absorption maxima at shorter wavelengths than closed isomers, which makes recording and deleting processes proceed independently by using recording and deleting beams at different wavelengths, respectively.

In this work, the relationship between their molecular structures and two-photon photochromic performances was discussed by synthesizing two typical chromene derivatives, 5a,9-dimethyl-5aH-benzo[b]chromene (**1**) and 7a,11-dimethyl-7aH-dibenzo[b,f]chromene (**2**). Compound **1** has the most simple chromene structure, and **2** has a similar structure as **1**, except for the additional condensation of a benzene ring onto the benzopyran ring. Fig. 2 shows molecular structures of their four possible isomers. In this paper, we first report on the photochromic performances of **1** and **2** by measuring ultraviolet (UV)–visible

\* Corresponding author. Tel.: +81-3-5734-2633; fax: +81-3-5734-2888.  
E-mail address: skawauch@polymer.titech.ac.jp (S. Kawauchi).



Fig. 1. Scheme of two-photon photochromic mechanism for chromene derivatives.

absorption and  $^1\text{H}$  nuclear magnetic resonance (NMR) spectral changes upon UV irradiation. Then, we evaluate the relative stabilities of closed, open-*Z*, open-*E* and bicyclo isomers for **1** and **2** by density functional theory (DFT) calculations. Combined with DFT calculations for 12a*H*-12a-methyl-naphtho[3,2]chromene (**3**), the most typical chromene derivative well exhibiting two-photon photochromism, we finally discuss the relationship between molecular structures and two-photon photochromic performances for chromene derivatives.

## 2. Experimental

### 2.1. General

All reactions in the experiment were carried out under a nitrogen ( $\text{N}_2$ ) atmosphere. Reagents were of analytical grade and were obtained from Kanto Chemical and Tokyo Kasei Industry. Solvents for synthesis were distilled just before use. Solvents for spectral measurements were of UV–infrared (IR) spectral grade.  $^1\text{H}$  and  $^{13}\text{C}$  NMR spectra were recorded on a JEOL GSX500 spectrometer operating at 500 MHz. All chemical shifts were referenced to tetramethylsilane (TMS) as an internal standard. Fourier transform infrared (FT-IR) spectra were recorded on a Shimadzu FTIR-8200 spectrophotometer.

### 2.2. Synthesis

5a,9-Dimethyl-5a*H*-benzo[*b*]chromene (**1**) and 7a,11-dimethyl-7a*H*-dibenzo[*b,f*]chromene (**2**) were synthesized according to the scheme, as shown in Fig. 3. First, 2-lithio-

*m*-xylene (**5**) was prepared from 2-bromo-*m*-xylene (**4**) with butyl lithium. Then, intermediate diol derivatives, **7** and **9**, were obtained by condensation of **5** with salicylaldehyde (**6**) and 2-hydroxy-1-naphthalenecarbaldehyde (**8**), respectively. Finally, the closed isomer of **1** (**1c**) and the open-*E* isomer of **2** (**2e**) were obtained by dehydration of **7** and **9** with anhydrous magnesium sulfate ( $\text{MgSO}_4$ ), respectively.

#### 2.2.1. $\alpha$ -(2-Hydroxyphenyl)-2,6-dimethylbenzyl alcohol (**7**)

At  $-75^\circ\text{C}$ , butyl lithium ( $2.5\text{ mol l}^{-1}$ , 20 ml, 0.05 mol) in hexane was added to a solution of 2-bromo-*m*-xylene (**4**) (8.328 g, 0.045 mol) in distilled tetrahydrofuran (THF) (20 ml) under a  $\text{N}_2$  atmosphere. The mixture was stirred at  $-75^\circ\text{C}$  for 2 h, followed by addition of a salicylaldehyde (**6**) (2.442 g, 0.02 mol) solution in distilled THF (30 ml). The mixture temperature was increased gradually to the range between 15 and  $20^\circ\text{C}$ . After the mixture was stirred in this temperature range for 24 h, the reaction was stopped by adding HCl ( $1\text{ mol l}^{-1}$ , 60 ml, 0.06 mol) and  $\text{H}_2\text{O}$  (50 ml). The products were extracted with ethyl acetate, dried by  $\text{MgSO}_4$ , and purified by column chromatography (silica gel, 200 mesh, 15/25, 30 cm, hexane/ethyl acetate: 3/1). Among the products, the component with  $R_f = 0.49$  on thin-layer chromatography (TLC) was collected. Recrystallization from a solution of hexane/ethyl acetate (5/1, v/v) yielded 2.961 g (65%) of **7** as a white crystalline powder.  $^1\text{H}$  NMR ( $\text{CDCl}_3$ ),  $\delta$  (ppm): 2.27 (s, 6H), 6.39–7.17 (m, 9H), 9.01 (s, 1 H).  $^{13}\text{C}$  NMR ( $\text{CDCl}_3$ ),  $\delta$  (ppm): 20.4 (s,  $-\text{CH}_3$ ), 76.3 (s, C–O), 120.8–133.7 (m, aromatic), 158.5 (s, aromatic C–O). IR (KBr): 3431, 3213, 3069, 2961, 1585, 1490, 1471, 1400, 1292, 1250 and  $1231\text{ cm}^{-1}$ .

#### 2.2.2. 5a,9-Dimethyl-5a*H*-benzo[*b*]chromene (**1**)

At  $85^\circ\text{C}$ , *p*-toluenesulfonic acid (TosOH) and anhydrous  $\text{MgSO}_4$  (1.44 g, 0.012 mol) were added to a solution of the white powder (**7**) (2.74 g, 0.012 mol) in distilled toluene (50 ml). The mixture was stirred at  $85^\circ\text{C}$  for 5 h under a  $\text{N}_2$  atmosphere. After filtration of  $\text{MgSO}_4$  and evaporation of toluene, the products were purified by column chromatography (hexane/ethyl acetate: 5/1). Among the products, the

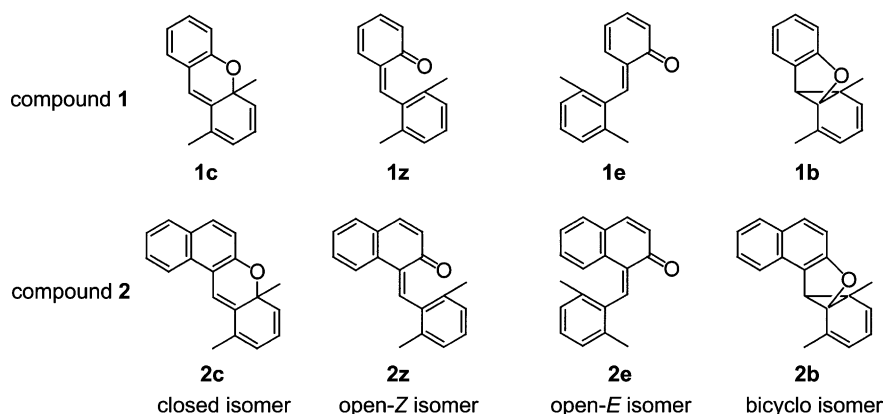
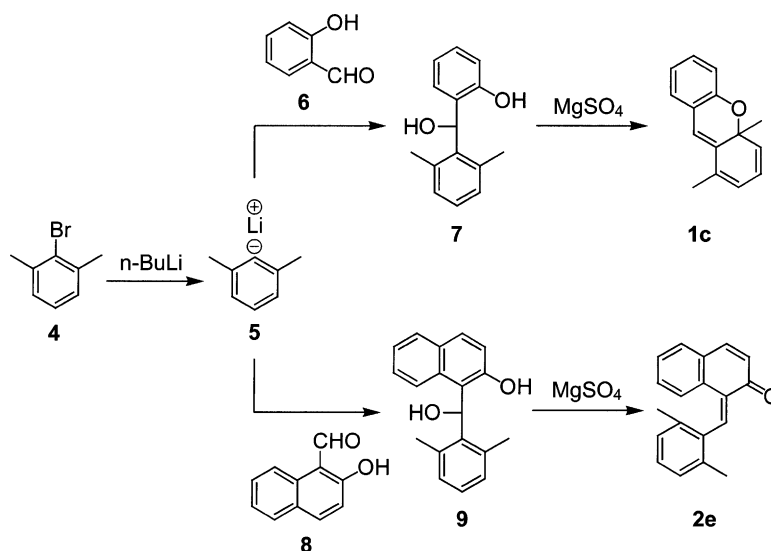


Fig. 2. Molecular structures of target chromene derivatives and their four possible isomers.

Fig. 3. Synthesis methods for **1** and **2**.

component with  $R_f = 0.21$  on TLC was collected. After evaporation of solvents, 2.39 g (95%) of **1c** was obtained as a white powder.  $^1\text{H NMR}$  ( $\text{CDCl}_3$ ),  $\delta$  (ppm): 2.10 (s, 3H), 2.62 (s, 3H), 6.51–7.23 (m, 8H).  $^{13}\text{C NMR}$  ( $\text{CDCl}_3$ ),  $\delta$  (ppm): 20.4 (s,  $-\text{CH}_3$ ), 22.8 (s,  $-\text{CH}_3$ ), 83.9 (s, C–O), 122.8–139.2 (m, aromatic), 162.3 (s, aromatic C–O). IR (KBr) 3067, 2966, 1585, 1472, 1454, 1375, 1290, 1238 and  $1041\text{ cm}^{-1}$ . Found: C, 85.36%; H, 6.94%. Calculated for  $\text{C}_{15}\text{H}_{14}\text{O}$ : C, 85.68%; H, 6.71%.

### 2.2.3. $\alpha$ -(2-Hydroxy-1-naphthyl)-2,6-dimethylbenzyl alcohol (**9**)

At  $-75^\circ\text{C}$ , butyl lithium ( $2.5\text{ mol l}^{-1}$ , 20 ml, 0.05 mol) in hexane was added to a solution of 2-bromo-*m*-xylene (**4**) (8.328 g, 0.045 mol) in distilled THF (20 ml) under a  $\text{N}_2$  atmosphere. The mixture was stirred at  $-75^\circ\text{C}$  for 2 h, followed by addition of a 2-hydroxy-1-naphthalenecarbaldehyde (**8**) (3.444 g, 0.02 mol) solution in distilled THF (30 ml). The mixture temperature was increased gradually to the range between 15 and  $20^\circ\text{C}$ . After the mixture was stirred in this temperature range for 24 h, the reaction was stopped and the products were extracted and purified by the same procedure described above for **7**. Among the products, the component with  $R_f = 0.53$  on TLC was collected. Recrystallization from a solution of hexane/ethyl acetate (10/1, v/v) yielded 3.313 g (56%) of **9** as a yellow crystalline powder.  $^1\text{H NMR}$  ( $\text{CDCl}_3$ ),  $\delta$  (ppm): 2.36 (s, 6H), 2.72 (s, 1H), 7.02–7.25 (m, 8H), 7.68–7.71 (m, 1H), 10.46 (s, 1H).  $^{13}\text{C NMR}$  ( $\text{CDCl}_3$ ),  $\delta$  (ppm): 20.1 (s,  $-\text{CH}_3$ ), 74.5 (s, C–O), 114.4–139.1 (m, aromatic), 154.9 (s, aromatic C–O). IR (KBr) 3285, 3020, 2921, 1626, 1605, 1468, 1418, 1231 and  $1061\text{ cm}^{-1}$ .

### 2.2.4. 1-(2,6-Dimethylbenzylidene)-2-oxo-1,2-dihydronaphthalene (**2**)

At  $85^\circ\text{C}$ , TosOH and anhydrous  $\text{MgSO}_4$  (1.32 g, 0.011 mol) were added to a solution of the yellow powder

(**9**) (3.032 g, 0.011 mol) in distilled toluene (50 ml). The mixture was stirred at  $85^\circ\text{C}$  for 5 h under a  $\text{N}_2$  atmosphere. The products were purified by the same procedure described above for **1**. Among the products, the component with  $R_f = 0.39$  on TLC was collected. Recrystallization from hexane yielded 2.10 g (73%) of **2e** as a yellow crystalline powder.  $^1\text{H NMR}$  ( $\text{CDCl}_3$ ),  $\delta$  (ppm): 2.12 (s, 6H), 6.44–6.47 (d, 1H), 6.97–7.48 (m, 8H), 8.18 (s, 1H).  $^{13}\text{C NMR}$  ( $\text{CDCl}_3$ ),  $\delta$  (ppm): 20.0 (s,  $-\text{CH}_3$ ), 126.6–145.2 (m, aromatic), 187.6 (s, aromatic C=O). IR (KBr) 3052, 2952, 2360, 1661, 1582, 1466, 1396, 1244 and  $1205\text{ cm}^{-1}$ . Found: C, 87.72%; H, 6.36%. Calculated for  $\text{C}_{19}\text{H}_{16}\text{O}$ : C, 87.66%; H, 6.15%.

## 2.3. Spectral investigations

Absorption spectral investigations were carried out outside the NMR spectrometer. UV–visible absorption spectra were recorded on a JASCO V-530 spectrometer. Transient absorption spectra were measured with a conventional laser flash photolysis system consisting of a XeCl excimer laser (Lumonics TE-860-4; 308 nm, 110 mJ per pulse, 10 ns per pulse) and a steady-state Xe lamp (Ushio UXL-300DO; 300 W) as the monitoring light source. Samples in hexane solution flowed through a cuvette of 40 mm optical path length in order to remove the influence of photoproduct and avoid sample heating. Transient absorption spectra were recorded on a JASCO V-550 spectrometer. A detailed description of this setup is reported elsewhere [15].

## 2.4. Molecular calculations

Ground state geometries of closed, open-*Z*, open-*E* and bicyclo isomers for **1–3** were optimized by the Becke's three-parameter hybrid DFT model [16] using the Lee–Yang–Parr correlation function [17] with the 6-31G\*

basis set [18] (denoted as B3LYP/6-31G\*). DFT calculations were implemented with GAUSSIAN 98 [19]. The total energy was corrected with the zero-point vibrational energy, and the total energy of each closed isomer was used as a reference to calculate the relative energies of others isomers for chromene derivatives, respectively. All the calculated geometries are equilibrium structures, which was confirmed by the normal mode analysis. The relative energies of these isomers calculated from DFT method were used to evaluate their relative stabilities. UV–visible absorption for **1–3** was calculated using random phase approximation (RPA) method after the geometry optimization by B3LYP/6-31G\*.

### 3. Results and discussion

#### 3.1. Photochromic performances of 5a,9-dimethyl-5aH-benzo[b]chromene (**1**)

Fig. 4 shows absorption spectral change of **1** in hexane. The original solution was colorless and had an absorption maximum ( $\epsilon = 1.15 \times 10^3 \text{ cm}^{-1} \text{ M}^{-1}$ ) at 267 nm. Irradiation of the colorless solution with UV light ( $\lambda = 254 \text{ nm}$ ) gave a yellow solution showing three absorption maxima at 378, 312, and 255 nm. The yellow solution then became colorless after being kept in the dark at room temperature for 2 days. During this bleaching process, the absorption maximum at 378 nm disappeared and the other two absorption maxima at 312 and 255 nm decreased, whereas a new absorption maximum at 275 nm can be seen. We further found that the yellow solution could also be bleached upon irradiation with UV light ( $\lambda > 325 \text{ nm}$ ).

Photoproducts of **1** during UV irradiation were investigated by measuring the  $^1\text{H}$  NMR spectral change in cyclohexane- $\text{d}_{12}$ . Upon irradiation with UV light ( $\lambda = 254 \text{ nm}$ ) for 10 min, three new proton peaks at 2.14 (s), 6.24 (d) and 8.04 ppm (s) separated from the original main

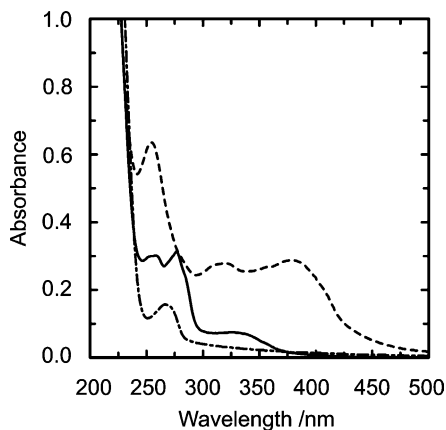


Fig. 4. Spectral change of **1** in hexane: original sample (dash-dotted line); upon irradiation with UV light ( $\lambda = 254 \text{ nm}$ ) (dashed line); after being kept in the dark for 2 days (solid line).

aromatic proton peaks. The former and the latter two are assigned to the methyl and aromatic protons of one keto isomer (i.e., either **1z** or **1e**), respectively. Further UV irradiation for 20 min gave rise to the formation and strengthening of two new peaks at 1.15 ppm (s) and 1.99 ppm (s). These two peaks are assigned to the methyl protons bounded to cyclopropane [11–14] and to cyclohexadiene rings, respectively, indicating the formation of **1b** upon continuous irradiation. The two peaks did not change after the solution was kept in the dark at room temperature for 1 day, but became weaker upon irradiation with UV light ( $\lambda > 325 \text{ nm}$ ). This suggests that **1b** is stable in the dark at room temperature, but readily converts to **1e** through **1z** upon photoirradiation.

To evaluate the relative stabilities of four isomers for **1**, we calculated their relative energies by DFT method. Fig. 5 shows the optimized ground state geometries of four isomers, as well as their relative energies and dipole moments. The relative energy sequence for **1** is  $1e < 1z \sim 1c < 1b$ . The differences in relative energies between the most unstable **1b** and the other three isomers are as large as more than  $60 \text{ kJ mol}^{-1}$ . Due to the high endothermicity and the large activation energy, the isomerization between **1b** and **1z** might be thermally prohibited, and only occur upon photoirradiation. In addition, **1c** is almost as stable as **1z**, but is less stable than **1e** by  $11.8 \text{ kJ mol}^{-1}$ . It is notable that the keto isomers (i.e., **1e** and **1z**) have larger dipole moments than **1c** and **1b**. Therefore, keto isomers might be destabilized in less polar solvents (benzene, hexane or cyclohexane- $\text{d}_{12}$ ), thereby changing the relative stability sequence of **1c** and keto isomers, because the differences in relative energies between **1c** and keto isomers are small (approximately  $10 \text{ kJ mol}^{-1}$ ).

Based on the analysis of  $^1\text{H}$  NMR spectra of photoproducts and DFT calculations for four isomers, we explain the photochromic reactions of **1** with the mechanism shown in Fig. 6. Irradiation of the closed isomer with UV light ( $\lambda = 254 \text{ nm}$ ) results in the formation of **1z**. Then, **1z** converts either to **1b** by strong or continuous irradiation, or to **1e** via thermal reaction if the irradiation is weak or stops. Therefore, the resulting yellow solution consists of **1e** exhibiting absorptions at 378, 312, and 255 nm and **1b** exhibiting absorption at 275 nm, possibly as well as trace quantities of **1z**. This explains why only one keto isomer, **1e**, was detected by absorption spectrum and  $^1\text{H}$  NMR. At this moment, however, the absorption peak at 275 nm corresponding to **1b** is completely hidden in the strong absorption peak at 255 nm corresponding to **1e**, thereby accounting for the invisibility of the absorption at 275 nm in the absorption spectrum of the yellow solution. Continuous irradiation gives the transformation from **1c** to **1b** through **1z**, resulting in the strengthening of  $^1\text{H}$  NMR peaks of **1b** at 1.15 and 1.99 ppm. When the yellow solution is kept in the dark at room temperature, **1e** returns to **1c** via thermal reaction through **1z**, whereas **1b** remains in the bleached solution. Therefore, the absorptions of **1e** at 378, 312, and 255 nm become weak, but that of **1b** at 275 nm remains unchanged. As a result, the hidden absorption of **1b** at 275 nm can be observed for the first

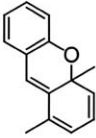
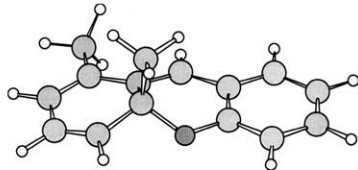
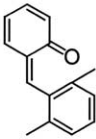
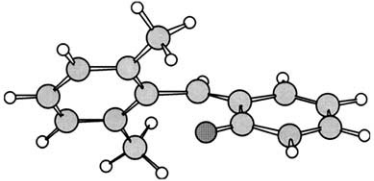
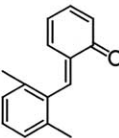
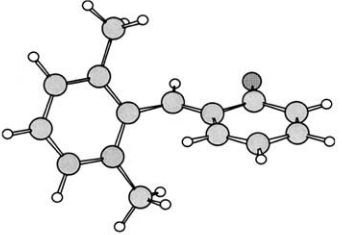
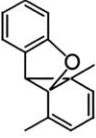
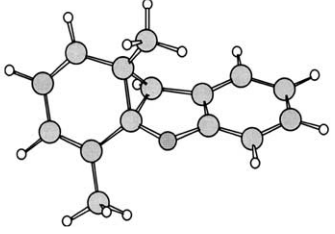
Molecular structure	Ground state geometry ● C ○ H ● O	Relative energy (kJ mol <sup>-1</sup> )	Dipole moment (Debye)
		0	1.28
		-0.3	2.73
		-11.8	3.42
		62.3	0.70

Fig. 5. Ground state geometries of four isomers for **1** optimized at the B3LYP/6-31G\* level: closed isomer; open-Z isomer; open-E isomer; bicyclo isomer.

time due to the weakening of the absorption of **1e** at 255 nm. This further accounts for the non-proportional decay of the overall spectrum shown in Fig. 4. On the other hand, both **1e** and **1b** revert to **1c** through **1z** upon irradiation with UV

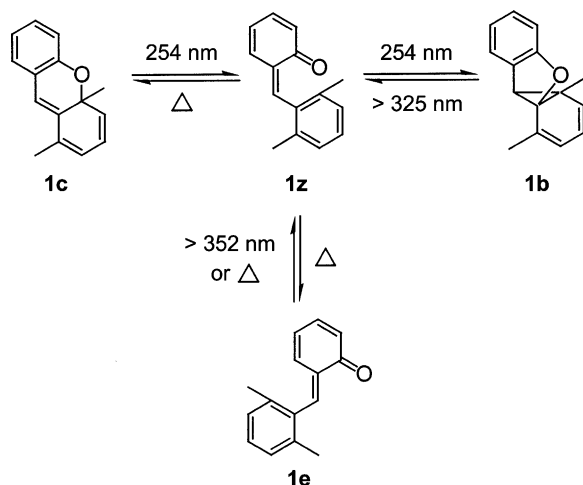


Fig. 6. Photochromic reaction mechanism of **1**.

light ( $\lambda > 325$  nm), which results in the bleaching of the yellow solution upon photoirradiation.

The relative energies of several isomers of **1** play an important role in the above mechanism. Compound **1z** preferentially converts to **1e** rather than to **1c** because **1e** is more stable than **1c** by 11.8 kJ mol<sup>-1</sup>. Although **1e** does not participate in two-photon photochromic reactions, it interferes with those reactions. Therefore, **1**, although showing two-photon photochromic reactions, does not have the non-destructive readout ability with an intensity of threshold, because of the formation of **1e**.

### 3.2. Photochromic performances of 7a,11-dimethyl-7aH-dibenzo[b,f]chromene (**2**)

The photochromic performances of **2** in hexane differ from those of **1**. Fig. 7 shows absorption spectral change of **2** in hexane. The original solution was yellow and its spectrum had two absorption maxima at 348 ( $\epsilon = 7.43 \times 10^3$  cm<sup>-1</sup> M<sup>-1</sup>) and 260 nm ( $\epsilon = 1.79 \times 10^4$  cm<sup>-1</sup> M<sup>-1</sup>). Upon irradiation with UV light ( $\lambda = 355$  nm), the absorption maximum at 348 nm shifted to a shorter wavelength



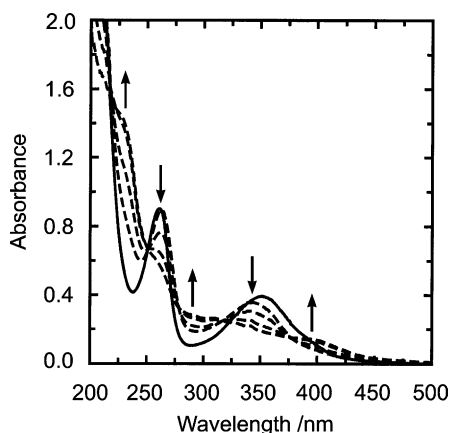


Fig. 7. Spectral change of **2** in hexane: original sample (solid line); upon continuous irradiation with UV light ( $\lambda = 355$  nm) (dashed line).

region ( $\lambda = 345$  nm) and the absorption maximum at 260 nm shifted to a longer wavelength region ( $\lambda = 265$  nm). Further irradiation resulted in the weakening of these new absorption maxima, and finally the flattening of absorption spectrum. Although the final absorption spectrum tailed more into the visible region, the solution appeared colorless, because the color change caused by such weak absorption is too small to be susceptible to our eyes. During this bleaching process, several isosbestic points were observed clearly at 251, 278, 316 and 373 nm in absorption spectrum, indicating the existence of an equilibrium reaction. However, the isosbistics are not good at longer wavelengths, implying a complicated reaction system besides the equilibrium reaction. In addition, the final products are not the same as the initial product that resulted in a peak shift (348–345 and 260–265 nm), because flattening the spectrum would not shift the absorption peaks in an opposite direction. The spectral change implies that **2** shows a more complex photoreaction mechanism rather than two-photon photochromic reactions.

Photoproducts of **2** during UV irradiation were investigated by measuring the  $^1\text{H}$  NMR spectral change in cyclohexane- $\text{d}_{12}$ . Upon irradiation with UV light ( $\lambda = 355$  nm), four new peaks at 2.15 (s), 6.09 (d), 7.69 (s), and 7.80 ppm (d) appeared, which slightly separated from the original peaks at 2.10 (s), 6.30 (d), 8.08 (s) and 7.23 ppm (d), respectively, in the  $^1\text{H}$  NMR spectrum. These new peaks are assigned to methyl protons, aromatic protons bounded to the carbonyl, olefinic protons, and aromatic protons bounded to naphthyl ring in keto isomers, respectively. The appearance of these new peaks indicates that photoirradiation led to the isomerization from one of the keto isomers (i.e., either **2e** or **2z**) to the other. Further irradiation gave rise to the strengthening of these new peaks, and the weakening of those peaks assigned to the original keto isomer. By integrating intensities of the two peaks at 2.10 and 2.15 ppm, more than 80% of the original keto isomer converted into the photo-generated keto isomer upon photoirradiation for

2 h. However, the appearance of some peaks at 1.57, 1.74, 2.01, 2.26, 2.45, 2.60, 2.94, and 3.18 ppm implies the formation of some unknown products resulting from photo- or thermal reactions upon prolonged irradiation. It is difficult to determine whether **2c** and **2b** were produced in this process only from the  $^1\text{H}$  NMR spectrum. Even if **2c** and **2b** are produced, their quantities must be limited because the peaks from 1.57 to 3.18 ppm were weak. When the colorless solution was kept in the dark at room temperature, the peak at 2.10 ppm that is assigned to the original keto isomer became stronger, while the one at 2.15 ppm that is assigned to the photo-generated keto isomer became weaker, which means that the photo-generated keto isomer returned to the original keto isomer via thermal reaction. This thermal isomerization proceeded so slowly that after 1 week, the solution only gave a ratio of 1:2 for the original and photo-generated keto isomers in the equilibrium mixture.

To evaluate the relative stabilities of four isomers for **2**, we calculated their relative energies by DFT method. Fig. 8 shows the optimized ground state geometries of four isomers, as well as their relative energies and dipole moments. The relative energy sequence for **2** is  $2e < 2z < 2c < 2b$ . The isomer with the lowest relative energy is **2e**, implying that the original keto isomer obtained from synthesis might be the open-*E* isomer. Compound **2c** is less stable than **2z** and **2e** isomers by 25.8 and 33.0  $\text{kJ mol}^{-1}$ , respectively. The difference in relative energies between **2z** and **2e** is only 7.2  $\text{kJ mol}^{-1}$ , whereas those between the most unstable **2b** and the other three isomers are as large as more than 60  $\text{kJ mol}^{-1}$ . Although the keto isomers (i.e., **2z** and **2e**) have larger dipole moments than **2c**, the relative stability sequence of **2c** and keto isomers does not seem to be readily changed by the destabilization effect of less polar solvents. This is because the differences in relative energies between **2c** and keto isomers might be too large to be completely compensated by the solvent effect.

To further understand the photochromic reaction process of **2**, the transient absorption spectrum of **2** in hexane was measured with a laser excitation at 355 nm (Fig. 9). Due to the short period of a single laser pulse (10 ns per pulse), the transient absorption spectrum at the moment when laser pulse stops should represent the photo-generated instant products, and the residue in the transient absorption spectrum should represent the photo-generated final products.

First, we consider the photo-generated instant products. Two absorption increases were observed at 420 and 280 nm, respectively, whereas one absorption decrease was observed at 360 nm. The absorption spectrum showing the isomerization between **2e** and **2z** in Fig. 7 does not give such a large absorption increase at 420 nm, implying that the photo-generated instant product cannot contain the photo-generated keto isomer. It is noteworthy that after the laser pulse was stopped, the absorptions at 420, 360, and 280 nm did not decay proportionally. By fitting these decays with one single-exponential function, it was found that the absorption at 420 nm decayed with a lifetime of

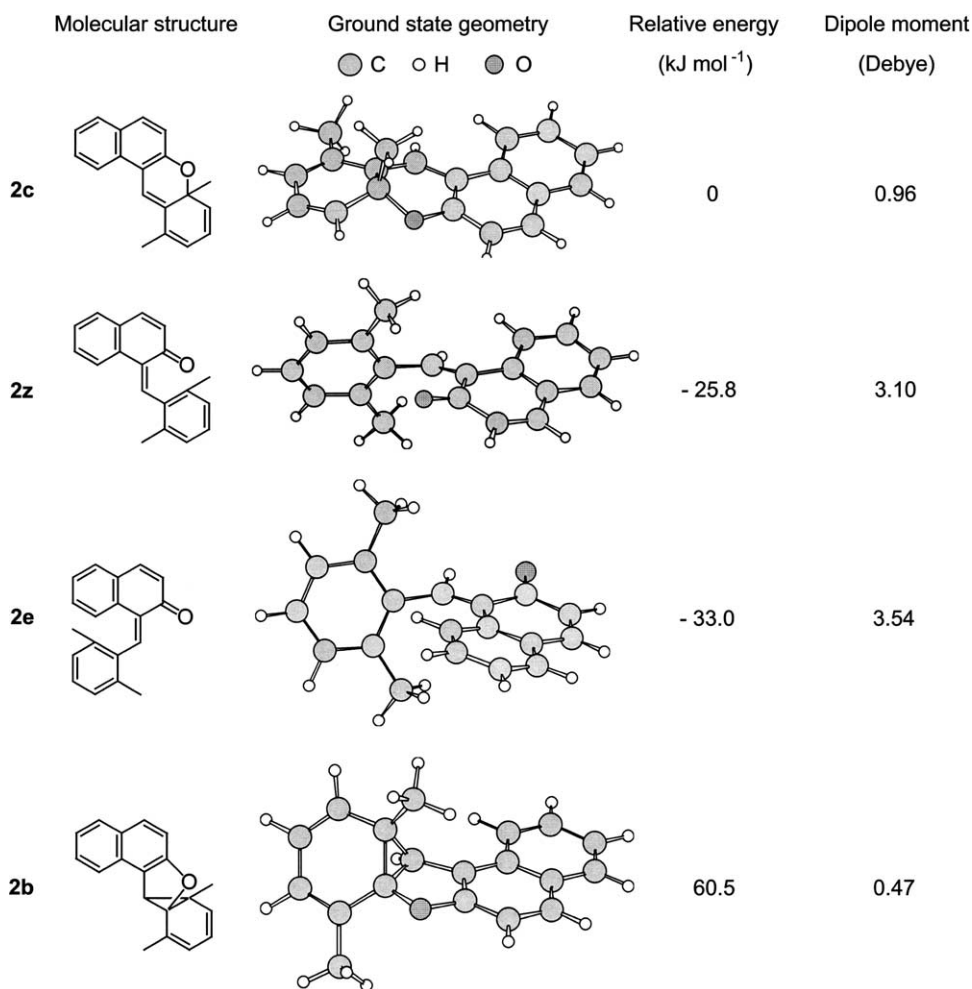


Fig. 8. Ground state geometries of four isomers for **2** optimized at the B3LYP/6-31G\* level: closed isomer; open-Z isomer; open-E isomer; bicyclo isomer.

approximately 50 ms, faster than those at 360 and 280 nm with a lifetime of approximately 400 ms, implying that the photo-generated instant products might consist of more than one species. Such short decay lifetimes of microsecond also

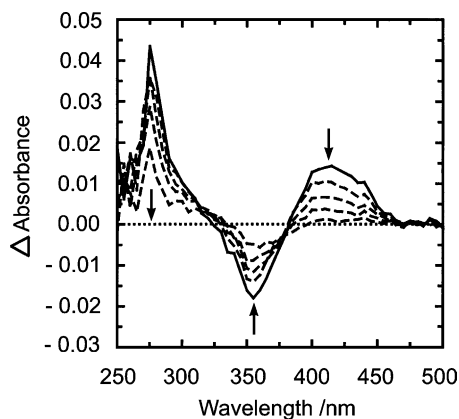


Fig. 9. Transient absorption spectrum of **2** in hexane with a laser excitation at 355 nm ( $4.0 \times 10^{-4}$  mol l<sup>-1</sup>) after: 0 ms (solid line); 22, 52, 92, 179 ms (dashed line) upon a single laser pulse.

imply that the photo-generated instant products cannot contain the photo-generated keto isomer, because it took 1 week for the 1:4 mixture of the original and photo-generated keto isomers to change to the 1:2 mixture in the dark. Therefore, we speculate that the photo-generated instant products might be a mixture of triplet states of the original keto isomer and other species, which remains to be identified by oxygen quenching experiment.

Next, we consider the photo-generated final products. The absorption increase at 420 nm returned to its original state, implying the photo-generated instant product resulting in the absorption increase at 420 nm returns to the original keto isomer during this decay process. However, the absorption increase at 280 nm and the absorption decrease at 360 nm did not return to their originate states in the transient spectrum, implying the formation of the new photo-generated final product different from the original keto isomer. The two absorptions at 360 and 280 nm in the transient spectrum match well with the absorption variation in these regions of the absorption spectrum showing the isomerization between **2e** and **2z** in Fig. 7. Therefore, it is reasonable to deduce

that the photo-generated final product showing absorption residues at 360 and 280 nm might be the photo-generated keto isomer.

Based on the above discussion, we explain the transient spectrum and its decay characters as the following. First, laser excitation leads to the formation of the triplet state of the original keto isomer, some of which converts to the triplet state of the photo-generated keto isomer within the time much shorter than microsecond. So, the transformation from the triplet state of the original keto isomer to that of the photo-generated keto isomer could not be detected by our transient spectral investigations. The triplet state of the original keto isomer returns to its ground state, accounting for the appearance of transient absorption increase at 420 nm and its decay with the lifetime of 50 ms. On the other hand, the triplet state of the photo-generated keto isomer converts to its ground state, accounting for the appearance of transient absorption decrease at 360 nm and increase at 280 nm, and their decays with the lifetime of 400 ms. The result of DFT calculations shows that the triplet states of **2e**, **2z**, and the transition state between them have the same relative energies of  $101.5 \text{ kJ mol}^{-1}$ . This zero-barrier character might ensure a fast transformation between two keto isomers within the time much shorter than microsecond, if neglecting side-reactions during the initial period of irradiation.

According to the analysis of  $^1\text{H}$  NMR spectra of photo-products, DFT calculations for four isomers, and the change of transient absorption spectrum, we propose the possible photochromic reaction mechanism for **2**, as shown in Fig. 10. Irradiation of **2e** with UV light ( $\lambda = 355 \text{ nm}$ ) results in the formation of **2z** through the triplet states of **2e** and **2z**. Most of **2z**, however, slowly returns to **2e** via thermal reaction and reaches the equilibrium. The appearance of isosbestic points

in the range between 251 and 373 nm in the absorption spectra (Fig. 7) is the evidence of the photo- and thermal isomerization equilibrium between **2e** and **2z**. On the other hand, continuous irradiation makes side-reactions (such as degradation) resulting from **2z** and/or **2e** prevail against the *E-Z* isomerization. Therefore, the absorption spectrum in Fig. 7 became flat. During this process, it is yet not clear whether **2c** and **2b** are produced or not. Nevertheless, we can conclude that upon irradiation, **2** mainly shows the isomerization between **2z** and **2e** as well as complex side-reactions.

It can be learned from the relative energies of several isomers for **2** that over stabilized keto isomers is responsible for the loss of two-photon photochromism. We do not further carry out a detailed research on the photoreaction mechanism of **2**, because our study focuses on the relationship between molecular structures and two-photon photochromism, not on the specific mechanism of photochromic reactions for an individual chromene derivative.

### 3.3. Relation between molecular structures and photochromic performances for chromene derivatives

The difference in photochromic performances of **1** and **2** can be understood from relative stabilities of their four isomers. By comparing the results from DFT calculations, we give some similarities in relative energies and dipole moments of four isomers for **1** and **2**. First, bicyclo isomers have the highest relative energies among four isomers, due to the steric cyclopropane ring in their molecular structures. In addition, although open-*E* isomers do not directly participate in two-photon photochromic reactions shown in Fig. 1, they do aggravate two-photon photochromic performances by interfering with two-photon photochromic reactions.

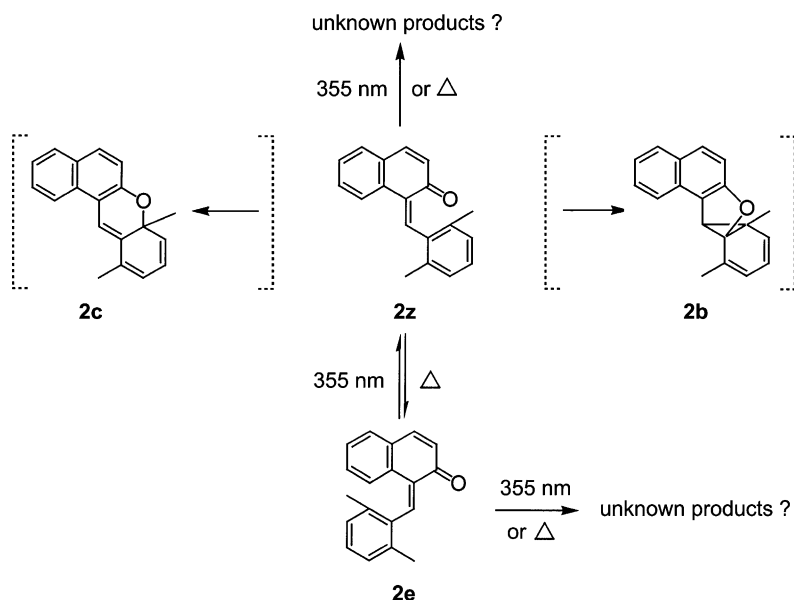


Fig. 10. Photochromic reaction mechanism of **2**.



Secondly, open-*E* isomers have similar ground state geometries as open-*Z* isomers, except for the relatively large steric hindrance due to methyl and ketone groups in open-*E* isomers. This makes open-*E* isomers a little more stable than open-*Z* isomers by approximately  $10 \text{ kJ mol}^{-1}$ . Finally, keto isomers have larger dipole moments than closed and bicyclo isomers. Therefore, the relative stability sequence of closed, open-*Z* and open-*E* isomers in less polar solvents (benzene, hexane or cyclohexane- $d_{12}$ ) depends on both their relative energies and the solvent effect.

Besides these similarities, there are some evident differences in thermal stabilities of four isomers for **1** and **2**. The relative energy sequence for **1** is open-*E* < open-*Z* ~ closed < bicyclo isomer, whereas for **2** it is open-*E* < open-*Z* < closed < bicyclo isomer. They are qualitatively similar, but quantitatively differ. For **1**, the closed isomer is almost as stable as the open-*Z* isomer, and less stable than the open-*E* isomer by  $11.8 \text{ kJ mol}^{-1}$ . On the contrary, for **2**, the closed isomer is less stable than the open-*Z* and open-*E* isomers by  $25.8$  and  $33.0 \text{ kJ mol}^{-1}$ , respectively.

Combining these similarities with differences, we classify the relative stability sequences of closed, open-*Z* and open-*E* isomers for chromene derivatives into three cases: (i) open-*E* < open-*Z* < closed isomer; (ii) open-*E* < closed < open-*Z* isomer; (iii) closed < open-*E* < open-*Z* isomer. The different sequences correspond to the different two-photon photochromic performances, as discussed in the following.

In case (i) (open-*E* < open-*Z* < closed isomer), represented by **2**, open-*E* isomers are the most stable, and closed isomers are the most unstable among three isomers. The differences in relative stabilities between closed and keto isomers are too large to be completely compensated by the destabilization of keto isomers in less polar solvents. As a result, the most stable, undesired open-*E* isomers interfering with two-photon photochromic reactions might be synthesized as the initial products. Therefore, the increased relative stability of keto isomers that results from the condensation of a benzene ring onto the benzopyran ring of **1** is of disadvantage to two-photon photochromism. Uchida and Irie [13] also reported that condensation of a benzene ring onto the naphthopyran ring of 12a*H*-12a-methyl-naphtho[3,2]chromene (**3**) results in the loss of two-photon reactivity, which agrees well with our results.

In case (ii) (open-*E* < closed < open-*Z* isomer), the effect of molecular structures of chromene derivatives on two-photon photochromic performances is more complicated than that in case (i). Although closed isomers become more stable, they are still less stable than open-*E* isomers. Compound **1** can be considered as this case approximately. We note that the differences in relative energies between keto isomers are not large (approximately  $10 \text{ kJ mol}^{-1}$ ), and the relative energies of closed isomers lie in this narrow region. Therefore, the destabilization effect of keto forms in less polar solvents might change the relative stability se-

quence of closed and open-*E* isomers, thereby increasing the uncertainty of two-photon photochromic performances. For **1**, although the closed isomer was synthesized as the initial product, the open-*E* isomer was produced during photochemical reactions, which results in its poor two-photon photochromic performances. Therefore, although the relative energy sequence in case (ii) exhibits the possibility of two-photon photochromism, it does not ensure the best two-photon photochromic performances.

In case (iii) (closed < open-*E* < open-*Z* isomer), closed isomers become the most stable among three isomers, which is of advantage to the best performances of two-photon photochromism. Moreover, the solvent effect further enhances the stability of closed isomers. Therefore, two things are ensured. One is that closed isomers are definitely synthesized as the initial products. The other is that photo-generated open-*Z* isomers preferentially revert to the most stable closed isomers via thermal reaction, rather than to the secondly stable open-*E* isomers. To confirm this inference, we calculated the relative energies of four isomers for 12a*H*-12a-methyl-naphtho[3,2]chromene (**3**), the most typical chromene derivative well exhibiting two-photon photochromism between the closed and bicyclo isomers [11], by DFT method. Fig. 11 shows the optimized ground state geometries of four isomers for **3**, as well as their relative energies and dipole moments. The relative energy sequence is closed < open-*E* < open-*Z* isomer, which is the same as our prediction. Therefore, chromene derivatives show the best two-photon photochromic performances only if closed isomers are more stable than keto isomers. In addition, the similarities in relative energies for **1** and **2** from DFT calculations are also feasible to **3**, such as the difference in relative energies between open-*E* and open-*Z* isomers, and the sequence of dipole moments for closed, keto, and bicyclo isomers.

It is noteworthy that the colorless **1c** with planar geometry gives the color **1e** that has non-planar geometry with hindered  $\pi$  conjugation, which is not consistent with the generally accepted concept that the more planar the molecule, the longer the wavelength of absorption maximum because of the increased  $\pi$  conjugation. This contradiction can be understood from two structural features of keto isomers for chromene derivatives. One is the charge-transfer effect resulting from the carbonyl group as a strong electron acceptor, which is effective in  $\pi$ -backbone systems, and resulting from the large dipole moment, which is effective in  $\sigma$ -backbone systems. Another is the enhanced contribution of  $n-\pi^*$  interactions to absorption spectrum at the existence of the hindered, non-planar  $\pi$  conjugation [20]. We calculated the absorption spectrum for **1–3** by RPA method. Table 1 shows the predicted absorption wavelength, oscillator strength, as well as configuration interaction (CI) coefficient of  $\pi-\pi^*$  and  $n-\pi^*$ , whose square indicates the extent of contribution to absorption. It can be seen that  $n-\pi^*$  transitions contribute more to absorption in keto isomers than in closed and bicyclo isomers, thereby resulting in the shifting

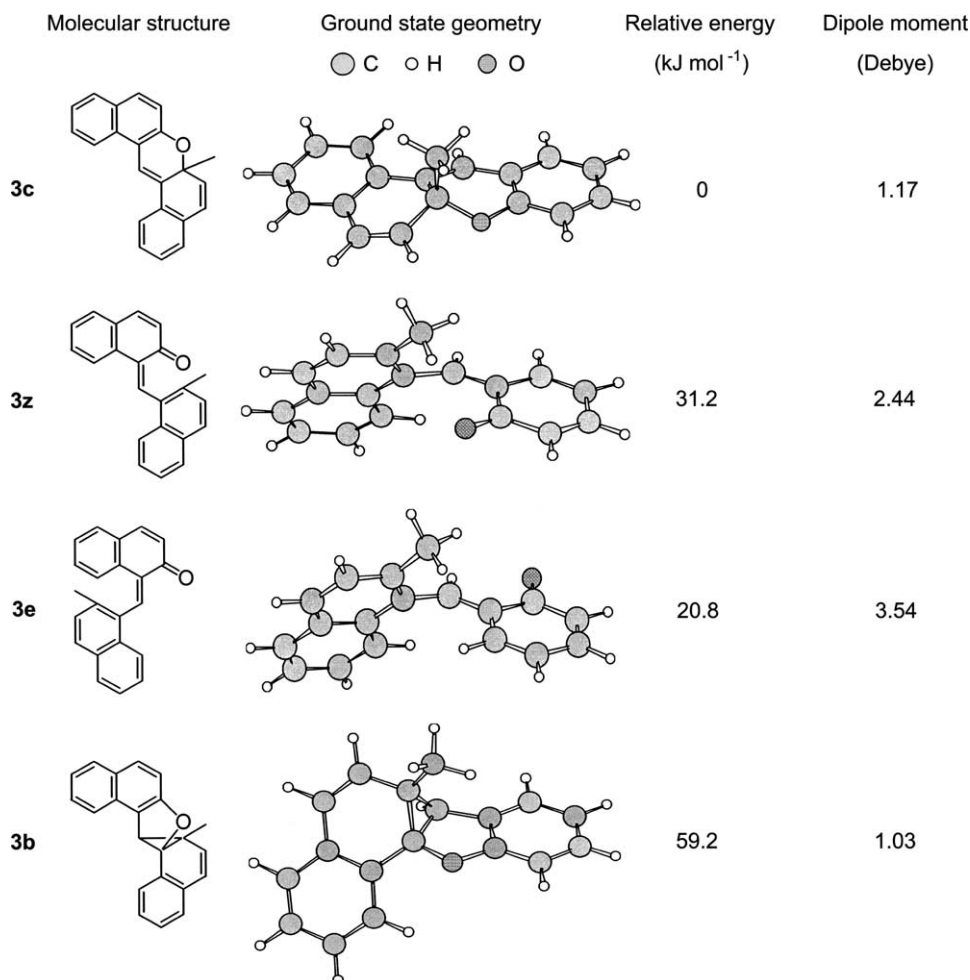


Fig. 11. Ground state geometries of four isomers for **3** optimized at the B3LYP/6-31G\* level: closed isomer; open-Z isomer; open-E isomer; bicyclo isomer.

Table 1  
Absorption maxima of four isomers for **1–3** predicted by RPA calculations

Compounds		Isomers			
		Closed	Open-Z	Open-E	Bicyclo
<b>1</b>	Wavelength (oscillator strength)	371 (0.168)	365 (0.090)	365 (0.157)	254 (0.166)
	Excitation orbital (CI coefficient)	56–57 (0.637)	53–57 (0.432) 55–57 (–0.286) 56–57 (–0.390)	53–57 (–0.251) 56–57 (0.585)	55–57 (–0.384) 56–58 (0.484)
<b>2</b>	Wavelength (oscillator strength)	400 (0.222)	423 (0.0230)	354 (0.093)	320 (0.079)
	Excitation orbital (CI coefficient)	69–70 (0.646)	65–70 (0.282) 69–70 (0.606)	68–70 (–0.291) 69–70 (0.581)	69–70 (0.654)
<b>3</b>	Wavelength (oscillator strength)	380 (0.235)	431 (0.153)	444 (0.174)	302 (0.109)
	Excitation orbital (CI coefficient)	65–66 (0.646)	63–66 (0.493) 65–66 (–0.400)	63–66 (–0.391) 65–66 (0.533)	65–66 (0.659)

of absorption maxima to the longer wavelength regions, although  $\pi$  conjugation is hindered due to the non-planar geometry of molecular structures. Such mechanism has been verified in a variety of compounds with non-planar geometry, such as naphthoquinone methide [20,21], indoaniline [22,23], and other chromene [14] derivatives.

#### 4. Conclusions

Two kinds of typical chromene derivatives, 5a,9-dimethyl-5aH-benzo[b]chromene (**1**) and 7a,11-dimethyl-7aH-dibenzo[b,f]chromene (**2**), were synthesized. They showed different photochromic performances in hexane upon

photoirradiation. Solution of **1** changed from colorless to yellow upon irradiation with UV light ( $\lambda = 254$  nm), and returned to colorless upon irradiation with UV light ( $\lambda > 325$  nm) or upon heating. Solution of **2**, however, only changed from yellow to colorless upon irradiation with UV light ( $\lambda = 355$  nm). Further analysis by measuring UV–visible absorption and  $^1\text{H}$  NMR spectra changes upon photoirradiation indicates that **1** showed the two-photon photochromic reaction, whereas the main photochemical reaction of **2** was the isomerization between the open-*E* and open-*Z* isomers. DFT calculations suggest that these different photochromic performances are attributed to the differences in thermal stabilities of closed, open-*Z* and open-*E* isomers for **1** and **2**. The increased relative stability of keto isomers is of disadvantage to two-photon photochromism. Combined with DFT calculations for 12a*H*-12a-methyl-naphtho[3,2]chromene (**3**), the most typical chromene derivative exhibiting two-photon photochromism, we conclude that chromene derivatives show the best two-photon photochromic performances only if closed isomers are more stable than open-*Z* and open-*E* isomers.

### Acknowledgements

We are grateful to Professor Koichi Mikami (Department of Chemical Engineering, Tokyo Institute of Technology) for helpful discussions about synthesis. We thank Professor Teijiro Ichimura and Dr. Tadashi Suzuki (Department of Chemistry, Tokyo Institute of Technology) for assisting with transient absorption spectral measurements. We also thank the Computer Center of Tokyo Institute of Technology for the use of SGI Origin 2000 and Compaq Alpha Server GS320 and the Research Center for Computational Science, Okazaki National Research Institutes for the use of SGI Origin 2800/3800. This work was supported in part by a Grant-in-Aid for Scientific Research from the Ministry of Education, Science, Sports and Culture of Japan.

### References

- [1] G.H. Brown, Photochromism, Wiley, New York, 1971.
- [2] Dürr, H. Bouas-Laurent, Photochromism, Molecules and Systems, Elsevier, Amsterdam, 1990.
- [3] H. Tada, J. Appl. Phys. 73 (1993) 489.
- [4] S.L. Gilat, S.H. Kawai, J.M. Lehn, J. Chem. Soc., Chem. Commun. (1993) 1439.
- [5] M. Irie, Jpn. J. Appl. Phys. 28 (1989) 215.
- [6] T. Tsujioka, M. Kume, M. Irie, Jpn. J. Appl. Phys. 35 (1996) 4353.
- [7] M. Nakagawa, M. Rikukawa, M. Watanabe, K. Sanui, N. Ogata, Bull. Chem. Soc. Jpn. 70 (1997) 737.
- [8] B.L. Ferigna, W.F. Jager, B. de Lange, J. Am. Chem. Soc. 113 (1991) 5468.
- [9] M. Irie, O. Miyatake, K. Uchida, J. Am. Chem. Soc. 114 (1992) 8715.
- [10] Y. Yokoyama, T. Yamane, Y. Kurita, J. Chem. Soc., Chem. Commun. (1992) 1722.
- [11] M. Uchida, M. Irie, J. Am. Chem. Soc. 115 (1993) 6442.
- [12] M. Uchida, M. Irie, Chem. Lett. (1992) 2257.
- [13] M. Uchida, M. Irie, Chem. Lett. (1995) 323.
- [14] M. Uchida, M. Kume, M. Irie, Bull. Chem. Soc. Jpn. 69 (1996) 1023.
- [15] S. Watanabe, M. Nagano, T. Suzuki, T. Ichimura, J. Photochem. Photobiol. A 137 (2000) 125.
- [16] A.D. Becke, J. Chem. Phys. 98 (1993) 5648.
- [17] C. Lee, W. Yang, R.G. Parr, Phys. Rev. B 37 (1988) 785.
- [18] P.C. Hariharan, J.A. Pople, Chem. Phys. Lett. 66 (1972) 217.
- [19] M.J. Frisch, G.W. Trucks, H.B. Schlegel, G.E. Scuseria, M.A. Robb, J.R. Cheeseman, V.G. Zakrzewski, J.A. Montgomery Jr., R.E. Stratmann, J.C. Burant, S. Dapprich, J.M. Millam, A.D. Daniels, K.N. Kudin, M.C. Strain, O. Farkas, J. Tomasi, V. Barone, M. Cossi, R. Cammi, B. Mennucci, C. Pomelli, C. Adamo, S. Clifford, J. Ochterski, G.A. Petersson, P.Y. Ayala, Q. Cui, K. Morokuma, D.K. Malick, A.D. Rabuck, K. Raghavachari, J.B. Foresman, J. Cioslowski, J.V. Ortiz, B.B. Stefanov, G. Liu, A. Liashenko, P. Piskorz, I. Komaromi, R. Gomperts, R.L. Martin, D.J. Fox, T. Keith, M.A. Al-Laham, C.Y. Peng, A. Nanayakkara, C. Gonzalez, M. Challacombe, P.M.W. Gill, B. Johnson, W. Chen, M.W. Wong, J.L. Andres, C. Gonzalez, M. Head-Gordon, E.S. Replogle, J.A. Pople, GAUSSIAN 98, Revision A.7, Gaussian, Inc., Pittsburgh, PA, 1998.
- [20] Y. Kubo, K. Yoshida, M. Adachi, S. Nakamura, S. Maeda, J. Am. Chem. Soc. 113 (1991) 2868.
- [21] Y. Kubo, M. Kuwana, K. Yoshida, Y. Tomotake, T. Matsuzaki, S. Maeda, J. Chem. Soc., Chem. Commun. 1 (1989) 35.
- [22] M. Adachi, Y. Murata, S. Nakamura, J. Org. Chem. 58 (1993) 5238.
- [23] M. Adachi, Y. Murata, S. Nakamura, J. Am. Chem. Soc. 115 (1993) 4331.